Calculation of mechanical properties of poly(*p*-phenylene terephthalamide) by atomistic modelling

G. C. Rutledge* and U. W. Suter†

Department of Chemical Engineering, Massachusetts Institute of Technology, Cambridge, MA 02139, USA and Institut für Polymere, Eidgenössische Technische Hochschule, CH-8092 Zurich, Switzerland

(Received 11 July 1990; revised 3 September 1990; accepted 17 September 1990)

The mechanical response of the solid state of a rigid rod polymer was evaluated through the static deformation of atomistic models. The calculations were applied to a set of polymorphs of poly(*p*-phenylene terephthalamide) (PPTA) previously deduced by molecular mechanics analysis. A series of simulated deformations of the minimum energy structures was used to predict all 21 independent elements each of the stiffness and compliance tensors. The significance of entropic and intermolecular potential contributions, in addition to the intramolecular potential contributions previously considered, to the accurate estimation of theoretical elastic moduli in such densely packed stiff chain polymer solids was elucidated. It was found that chain packing and entropy, or thermal motion, both have a significant effect on the fibre tensile modulus, but that they are of opposite sign and partially compensate. Elastic properties of aramid fibres were estimated by symmetrizing the single crystal elastic tensors in the limits of uniform strain and stress to yield Voigt and Reuss bounds, respectively, for the elastic moduli. For one structure of PPTA (closely resembling the crystallographically determined modification I) the calculated extensional, transverse, and torsional moduli are in the ranges 220–290, 5.2–19 and 4.1–12 GPa, respectively, in good agreement with observed values.

(Keywords: poly(*p*-phenylene terephthalamide); modelling; elasticity; crystal moduli; fibre moduli)

INTRODUCTION

Previous efforts at modelling of crystalline polymers tend to fall into two categories: predictions of elastic properties of known crystal forms, or derivation of structural and thermodynamic properties. For elastic constants, it has been common to assume that it is the response of potential energy to deformation that dominates elastic behaviour in crystals. As early as 1967 Anand[1] applied the concepts of atom-based force fields to predict the elastic constants for a known structure of orthorhombic polyethylene. McCullough[2] first developed a matrix technique for representing crystalline assemblies of chains of fixed conformation, with consideration of certain chain defects (e.g. chain kinking or folding). Elastic constants in polyethylene were studied by considering potential energy interactions within a single chain and between selected nearest neighbour chains in a given orthorhombic assembly. However, minimization of the potential energies with respect to either intramolecular or intermolecular parameters was not attempted. Tashiro *et al.*[3–5] also reported a method for the calculation of the three dimensional elastic moduli of assemblies of chains. This method took advantage of a priori crystal symmetries to expedite calculations and was applied to polyethylene (PE), poly(vinyl alcohol) and nylon 6. Tripathy *et al.*[6] dealt with the prediction of crystalline packing of chain molecules by minimizing the intermolecular interaction energies of assemblies of chains of fixed conformation using a formalism for the single chain which enabled the calculation of interactions between infinitely long chains. In this case, the polymers studied were PE and poly(vinylidene fluoride). However, this formalism was not amenable to extension to three dimensions.

More recently, Sorensen *et al.*[7,8] have incorporated the simultaneous minimization of packing energy with respect to both intramolecular conformation and intermolecular packing parameters, a feature important to the prediction of structure at solid state densities. These authors went on to deduce elastic constants, using the second derivative matrix of potential energy with respect to the independent variables at the minimum energy configuration, and vibrational dispersion curves, from which the thermodynamic quantities were calculated. Again, application to PE and poly(oxymethylene) showed remarkably good agreement between calculated and experimental values for packing geometry and lattice energy, and reasonable agreement for elastic constants and heat capacities between 50°C and 350°C.

Despite this considerable attention to simulations of flexible chain aliphatic polymers, there have been no reports of application of these methods to the case of rigid-rod polymers. Flory and co-workers[9,10] addressed the question of conformational energetics in *p*-phenylene polyamides and polyesters, with subsequent predictions of chain persistence lengths. Tashiro *et al.*[11] also performed single chain calculations on the three relevant aramids, poly(*p*-benzamide) (PBA), poly(*m*-phenylene isophthalamide), and poly(*p*-phenylene terephthalamide)

* To whom correspondence should be addressed at: Institut für Polymere, Eidgenössische Technische Hochschule, CH-8092 Zürich, Switzerland

† Present address: IRC in Polymer Science and Technology, University of Leeds, Leeds LS2 9JT, UK

0032-3861/91/122179-11

(PPTA), in order to elucidate conformational energetics and tensile moduli, based on the assumption that intermolecular effects contribute negligibly to axial moduli, with reasonable success. Both groups produced parameterized force fields to describe the conformational behaviour of the isolated chain and, in the latter case, its response to extensional deformation. Northolt and van Aartsen have also applied valence force field calculations to the estimation of axial, transverse and shear moduli[12]. However, in the solid state the environment is both conformationally constrained and densely packed. Under such strong opposing forces, one cannot expect to decouple the problems associated with the possibly antagonistic criteria for optimization of chain conformation and long range crystallinity regularity. It is especially important to recognize that intermolecular forces may be sufficient to induce changes in chain conformation and, by so doing, influence the intramolecular interactions. Conflicts between conformational intramolecular constraining forces and crystallographic intermolecular constraining forces are sufficient to induce the formation of non-crystallographic characteristics, e.g. non-rational helices or helix discommensurations such as those proposed by Saruyama *et al.*[13].

We have recently introduced an atomistic modelling approach for assemblies of oriented polymer chains in a pseudocrystalline matrix[14]. This model, though developed independently of that introduced earlier by Sorensen *et al.*[7] possesses many of the important features of that method, including the completely general description of chain packing in three dimensions and the simultaneous consideration of both intramolecular and intermolecular degrees of freedom. However, the current model allows in addition the deviation from perfect translational periodicity of lattice points along the chain contour and thus does not impose rigorous lattice crystallinity within the explicitly modelled region of the multichain construction. The constraint of perfect crystallinity and the translational periodicity of atomic positions implied thereby is imposed only for chains outside of the nearest neighbour shell surrounding the reference chain (i.e. a modified domain consisting of the parent chain and its nearest neighbours, embedded within a 'crystalline universe', composed of the next nearest neighbour shell and chains more distant from the reference chain). This model is especially appropriate to the description of polymeric solids, where the development of true crystallinity over large distances may be in conflict with the preferred conformational behaviour of the covalently bonded chain contour itself, which must intersect many 'unit cells'. We have previously presented results concerning the determination of three-dimensional structure in PPTA. This paper addresses the response of atomic structure to imposed deformation and the estimation of both the single crystal and the axially symmetric polycrystalline elastic constant matrices for PPTA.

THERMODYNAMIC ANALYSIS

Classical thermodynamics of deformation

Thermodynamic stability of structure is defined by minimization of the free energy with respect to the degrees of freedom describing the structure; as such, it is composed of both an internal energy contribution (potential and kinetic) and an entropic contribution. (It is common practice in molecular mechanics methods to consider the relative stability of different geometries solely in terms of a minimum potential energy criterion; the elastic constants are then calculated from the changes in potential energy upon deformation, corresponding to zero point elastic constants.) We take as our starting point the second derivatives of the Helmholtz free energy, A, with respect to deformation strain of a small volume element V_0:

$$A = U - TS \tag{1}$$

$$\mathrm{d}A = \mathrm{d}U - T\,\mathrm{d}S \quad \text{for isothermal deformations} \tag{2}$$

The elements of the fourth order elastic stiffness tensor, C_{LMNK}, are defined as:

$$\partial^2 A/\partial\varepsilon_{LM}\,\partial\varepsilon_{NK}|_o = V_o C_{LMNK} \tag{3}$$

where the elements of the Lagrangian ('material') strain tensor ε_{LM} are defined using:

$$2\varepsilon_{LM} = \partial u_L/\partial x_M + \partial u_M/\partial x_L + \sum_{I=1}^{3} \partial u_I/\partial x_L\,\partial u_I/\partial x_M \tag{4}$$

$\mathbf{u} = (u_1, u_2, u_3)$ is the displacement vector describing deformation. The subscript o indicates the minimum internal energy (i.e. reference) structure. The subscript LM refers to change of the L surface (i.e. a plane perpendicular to the L direction) in the M direction. For small deformations, we may neglect the terms of the second order in displacement.

Consider first an arbitrary elastic solid subjected to an arbitrary isothermal small deformation. Expanding the internal energy U into a Taylor series about the undeformed state and neglecting terms higher than second order, one obtains an expression based on the formulation of Weiner[15] and similar to that derived by Theodorou and Suter[16] for the difference in internal energy per structural repeat unit between the deformed state and the ground state:

$$\mathrm{d}U = U_{def} - U_o$$

$$\mathrm{d}U = \Sigma_{LM} M_{ru}(\sigma_{LM}/\rho_o + C_\varepsilon T\gamma_{LM})\varepsilon_{LM} + \frac{1}{2}\Sigma_{LM}\Sigma_{NK}(M_{ru}/\rho_o)[C_{LMNK} - T(\partial C_{LMNK}/\partial T)]\varepsilon_{LN}\varepsilon_{NK} \tag{5}$$

Here ρ_o is the density, M_{ru} is the molar mass of the repeat unit, and C_ε is the heat capacity at constant strain. The elements σ_{LM} of the material stress tensor and γ_{LM} of the Grüneisen tensor are defined by:

$$\partial A/\partial\varepsilon_{LM}|_{[LM],o} = V_o\sigma_{LM} \tag{6}$$

$$\partial S/\partial\varepsilon_{LM}|_{[LM],o} = \gamma_{LM} C_\varepsilon \rho_o V_o \tag{7}$$

In our notation, the subscript [LM],o signifies that all variables, temperature inclusive, except for that indicated within the parentheses are held constant. This notation will be simplified in the following to the reference structure subscript o, with variation of only those elements indicated by partial derivatives implied. In our simulations the zero-strain dimensions are included as variables in the energy minimization. The energy is, therefore, minimized with respect to density; hence the first term in equation (5), the internal residual stress[16], is zero. The second term reflects the connection between the elastic stiffnesses and the second derivatives of internal energy with respect to strain. To assess the relative importance of the contributions of internal

energy and entropy to the elatic constants, the second derivative of Helmholtz energy with respect to strain is evaluated:

$$V_o C_{LMNK} = \partial^2 A/\partial\varepsilon_{LM}\,\partial\varepsilon_{NK}|_o = \partial^2 U/\partial\varepsilon_{LM}\,\partial\varepsilon_{NK}|_o - T\,\partial^2 S/\partial\varepsilon_{LM}\,\partial\varepsilon_{NK}|_o \quad (8)$$

Entropic effects are relatively unimportant if:

$$|T(\partial^2 S/\partial\varepsilon_{LM}\,\partial\varepsilon_{NK})|_o/(\partial^2 A/\partial\varepsilon_{LM}\,\partial\varepsilon_{NK})|_o| \ll 1 \quad (9)$$

or

$$|T(\partial C_{LMNK}/\partial T)/C_{LMNK}|_o| = |\partial \ln C_{LMNK}/\partial \ln T|_o| \ll 1 \quad (10)$$

Evaluation of this inequality requires data for the elastic stiffnesses as functions of temperature at constant strain levels. Because such data at constant strain is generally difficult to obtain, this criterion has been re-expressed in terms of constant stress derivatives[16]:

$$|(T/C_{LMNK})[(\partial C_{LMNK}/\partial T)|_\sigma - \Sigma_{LM}\Sigma_{NK} T\alpha_{NK}(\partial C_{LMNK}/\partial\sigma_{LM})|_{[LM],\sigma;T}]| \ll 1 \quad (11)$$

Here, the subscript σ indicates constant stress derivatives, while $[LM],\sigma$ indicates constant stress except for derivatives with respect to LM. For the general crystal lattice, where elastic response to imposed stress is generally anisotropic, one requires the complete thermal expansion tensor α, expressed alternatively by the Grüneisen tensor component γ_{LM}:

$$\alpha_{PQ} = (C_\varepsilon/V_o)\Sigma_{LM} S_{PQLM}\gamma_{LM} \quad (12)$$

Thus to evaluate the significance of entropic contributions to the elastic constants, one generally requires either the temperature coefficients at constant strain or the temperature coefficients at constant stress and the elements of the thermal expansion or the Grüneisen tensor. Unfortunately, the complete thermal expansion tensor or the Grüneisen tensor are rarely available for the anisotropic solid. One must usually settle for a few select elements, typically the diagonal elements, of either tensor.

With respect to the particular case of the stiff chain polymer, Ii *et al.* in a series of papers[17–19] reported lattice thermal expansion data and some thermomechanical properties for PPTA and PBA aramid fibres obtained by means of X-ray analysis of the crystal lattice spacings under given axial (*c*-axis) loadings. Relevant properties which may be deduced from this work are reproduced in *Table 1*. Based on these values, we may calculate the stiffness criterion for $\partial^2 A/\partial\varepsilon_{33}^2$, assuming that only the axial stiffness constant C_{3333} is significantly affected by the introduction of an axial stress σ_{33}. In the second term of equation (11), one would expect that for such oriented chains $\partial C_{3333}/\partial\sigma_{33}$ should far exceed all other $\partial C_{LMNK}/\partial\sigma_{LM}$ due to the deformation of internal bond lengths, angles and torsions required by an imposed stress in this direction, rather than the deformation of weaker intermolecular interactions allowed under stress in the other directions; the possible exception in the aramid case is $\partial C_{1111}/\partial\sigma_{11}$, which involves deformation of hydrogen bonds. However, the fact that C_{3333} should also be much greater than the other moduli, and that α_{11} and α_{22} are positive and thus would offset somewhat the negative α_{33} contribution, should ensure that the estimate calculated below is a worst case scenario:

$$|(T/C_{3333})[\partial C_{3333}/\partial T|_\sigma - T\alpha_{33}\,\partial C_{3333}/\partial\sigma_{33}|_T]| = 0.27 \text{ (PPTA)}, \quad 0.32 \text{ (PBA)} \quad (13)$$

These numbers imply that the true modulus of PPTA fibres is smaller than the value estimated from internal energy contributions alone, but is at least 79% of this value, while for PBA the corresponding lower limit is 76%.

Table 1 Thermomechanical properties of PPTA and PBA[a]

	PPTA	PBA
α_{11} (K^{-1})	8.3×10^{-5}	7.0×10^{-5}
α_{22} (K^{-1})	4.7×10^{-5}	4.1×10^{-5}
α_{33} (K^{-1})	-2.9×10^{-6}	-7.7×10^{-6}
$C_{3333}\approx 1/S_{3333}$ (at 298 K) (GPa)	168	188
$\partial C_{3333}/\partial T\|_{\sigma 33=0.5\,GPa} \approx -S_{3333}^{-2}\,\partial S_{3333}/\partial T\|_{\sigma 33=0.5\,GPa}$ (GPa K^{-1})	−0.181	−0.247
$\partial C_{3333}/\partial\sigma_{33}\|_{300K} \approx -S_{3333}^{-2}\,\partial S_{3333}/\partial\sigma_{33}\|_{300K}$	59	32

[a] From Ii *et al.*[17–19]

Statistical mechanics of deformation

Alternatively, in order to understand the contributions to the macroscopic thermodynamic properties of changes at the atomic scale, we may recast these state variables in terms of the canonical partition function for an N body system:

$$Q(N, V, T) = \sum_j \exp[-\beta E_j(N, V)] \quad (14)$$

where $\beta = 1/kT$ and the E_j are the total (free) energies of the states j available to the system. The thermodynamic state variables then become:

$$A = -kT \ln Q \quad (15)$$

$$U = kT^2\,\partial \ln Q/\partial T|_{N,V} \quad (16)$$

$$S = kT\,\partial \ln Q/\partial T|_{N,V} + k \ln Q \quad (17)$$

For a system of distinguishable particles, such as the atoms in a crystal lattice, the canonical partition function may be approximately decomposed into factors for additional treatment by either classical or quantum mechanical methods:

$$Q(N, V, T) = q_{trans}q_{rot}q_{vib} = Q_{class}Q_{quant} \quad (18)$$

Now, we choose to treat the crystal lattice in the vicinity of its minimum internal energy configuration as a regular structure of discrete lattice points at which are located the N bodies (or atoms) of the system; each body vibrates about its local lattice point. The total internal energy may then be expressed as a function of an arbitrary set of orthogonal structure-defining variables $\{s\}$ as a Taylor series expansion about the minimum energy configuration $\{s\} = \{s_o\}(\Delta s_i \in \{\Delta s\} \equiv \{s - s_o\})$:

$$U(\{s\}) = U(\{s\} = \{s_o\}) + \sum_{i=1}^{3N} \partial U/\partial\Delta s_i|_o\,\Delta s_i + \frac{1}{2}\sum_{i=1}^{3N}\sum_{j=1}^{3N} \partial^2 U/\partial\Delta s_i\,\partial\Delta s_j|_o\,\Delta s_i\,\Delta s_j \quad (19)$$

where the first term, the potential energy at the minimum, is a function only of the 'soft' variables and will be referred to hereafter as U_{min}^{pot}, and the second and third terms,

indicative of structural mobility, are functions of vibratory displacements about this static minimum, due either to oscillations in such 'hard' variables as bond lengths and bond angles or small oscillations in soft variables such as bond torsion or interchain distance, which are further assumed to be independent of $\{s_o\}$.

The positions described by the vector of change $\{\Delta s\}=\{0\}$ correspond to the minimum energy configuration, where by definition for a state in detailed mechanical equilibrium $\partial U/\partial(\Delta s_i)|_o=0$. The quadratic term represents a set of coupled harmonic oscillators. By next assuming that the crystal behaves as a large polyatomic molecule whose atoms occupy lattice points connected by 'springs', and introducing normal coordinate analysis, one may decompose the system into a set of independent oscillators, characterized by $3N$ (for large N) normal mode vibration frequencies v_j, each contributing its own component $q_{vib,j}$ to the quantized portion of the partition function. Equating $U(\{s\})$ with the set of energies E_j available to the system in the vicinity of the lattice minimum and substituting the independent partition functions $q_{vib,j}$ for the component oscillators in the quadratic term, one obtains[20]:

$$Q(N, V, T)=\exp(-\beta U_{min}^{pot})\prod_{j=1}^{3N} q_{vib,j} \tag{20}$$

where

$$q_{vib,j}=\exp(-\beta h v_j/2)/[1-\exp(-\beta h v_j)] \tag{21}$$

For the Helmholtz free energy and its second derivatives, this yields:

$$A=U_{min}^{pot}+kT\sum_{j=1}^{3N}\ln(q_{vib,j}) \tag{22}$$

$$\partial^2 A/\partial\varepsilon_{LM}\,\partial\varepsilon_{NK}|_o=\partial^2 U_{min}^{pot}/\partial\varepsilon_{LM}\,\partial\varepsilon_{NK}|_o + kT\sum_{j=1}^{3N}\partial^2\ln(q_{vib,j})/\partial\varepsilon_{LM}\,\partial\varepsilon_{NK}|_o \tag{23}$$

For the calculation of elastic stiffnesses, our interest lies in the term $\partial^2 A/\partial\varepsilon_{LM}\,\partial\varepsilon_{NK}|_o=VC_{LMNK}$. Clearly, if the normal mode frequencies are independent of deformation in the small deformation regime, then the second term on the right-hand side vanishes and $(\partial^2 A/\partial\varepsilon_{LM}\,\partial\varepsilon_{NK})$ may be replaced by $(\partial^2 U_{min}^{pot}/\partial\varepsilon_{LM}\,\partial\varepsilon_{NK})$, suggesting that thermal oscillations make at most a minor contribution to elastic response; this is the strict harmonic approximation. Thus for evaluation of the significance of contributions of thermal vibrations to elastic stiffnesses, one requires normal mode vibrational frequencies for both deformed and undeformed structures. Applying a criterion for significance of thermal motion contributions analogously to the one given in equation (9), one finds that the neglect of thermal motion is inconsequential if:

$$N_o kT\sum_{j=1}^{3N}\partial^2\ln(q_{vib,j})/\partial\varepsilon_{LM}\,\partial\varepsilon_{NK}|_o/NV_oC_{LMNK}\ll 1 \tag{24}$$

or

$$(N_o/\beta NV_oC_{LMNK})\sum_{j=1}^{3N}h\beta(\tfrac{1}{2}+\Lambda)\partial^2 v_j/\partial\varepsilon_{LM}\,\partial\varepsilon_{NK}|_o - (h\beta)^2(\Lambda+\Lambda^2)\,\partial v_j/\partial\varepsilon_{LM}|_o\,\partial v_j/\partial\varepsilon_{NK}|_o\ll 1 \tag{25}$$

where

$$\Lambda=1/[\exp(h\beta v_j)-1] \tag{26}$$

Data presented below leads one to assume that:

(i) $\partial v_j/\partial\varepsilon_{LM}|_o=K_v$, a constant for all j, LM and
(ii) $\partial^2 v_j/\partial\varepsilon_{LM}\,\partial\varepsilon_{NK}|_o=0$ for all j, LM, NK

With these assumptions, a simplified criterion is:

$$-(N_o/\beta NV_oC_{LMNK})(h\beta K_v)^2\sum_{j=1}^{3N}(\Lambda+\Lambda^2)\ll 1 \tag{27}$$

For large N, one may approximate the summation by introducing a distribution function $g(v)$ for the normal mode frequencies and integrate over all frequencies:

$$-(N_o/\beta NV_oC_{LMNK})(h\beta K_v)^2 \times\int_0^\infty \exp(h\beta v)g(v)/[\exp(h\beta v)-1]^2\,dv\ll 1 \tag{28}$$

where normalization requires that

$$\int_0^\infty g(v)\,dv=3N \tag{29}$$

It only remains to specify the distribution function $g(v)$ which describes the complete set of individual frequencies. Unfortunately, complete distributions are not generally available. Most of these frequencies are not due to the vibrations of single atoms or a few atoms, but are concerted (harmonic) motions of many or all atoms. The normal frequencies of a crystal vary from essentially zero to some value of the order of 10^{13} cycles s^{-1} (ref. 20). We may proceed by introducing the same approximations for the normal mode vibrations of a crystal as have been employed so successfully in the prediction of low temperature heat capacities, namely the Einstein and Debye approximations:

Einstein approximation. It is assumed that each normal mode has the same frequency v_E, i.e. each member of the lattice sees the same environment and acts as an independent oscillator:

$$g_E(v)=3N\,\delta(v-v_E) \tag{30}$$

which, when substituted into equations (28) and (29), yields:

$$\left|-(3N_o/\beta V_oC_{LMNK})(h\beta K_v)^2 \times\{\exp(h\beta v_E)/[\exp(h\beta v_E)-1]^2\}\right|\ll 1 \tag{31}$$

The lower v_E is, the larger is the left-hand side of equation (31).

Debye approximation. It is reasoned that only low frequencies, up to a characteristic frequency v_D, are important; those long wavelength oscillations are insensitive to the detailed atomic character of the solid and may be calculated by assuming that the crystal is a continuous elastic body. This leads to:

$$\begin{aligned} g_D(v)&=9Nv^2/v_D^3 \qquad 0\leqslant v\leqslant v_D \\ &=0 \qquad\qquad\quad v>v_D \end{aligned} \tag{32}$$

which, when substituted into equations (28) and (29) and making the substitution $x=h\beta v$, leads to:

$$\left|-(3N_o/\beta V_oC_{LMNK})(K_v^2/h\beta v_D^3) \times\int_0^{h\beta v_D} x^2\exp(x)/[\exp(x)-1]^2\,dx\right|\ll 1 \tag{33}$$

Table 2 Strain dependence of Raman frequencies in PPTA[a]

Frequency (cm^{-1})	$\partial\nu_j/\partial\varepsilon_{33}$ (cm^{-1} $\%^{-1}$)	$\Lambda+\Lambda^2$ ($\times 10^4$)
1649.5	-2.2 ± 0.2	3.65
1613.5	-4.4 ± 0.2	4.33
1519.2	-4.2 ± 0.7	6.82
1330.9	-3.4 ± 0.3	16.90
1280.1	-3.6 ± 0.3	21.50
1183.7	-0.5 ± 0.3	34.30

[a] From Galiotis *et al.*[21]

which may be integrated numerically for a given ν_D. The lower ν_D is, the larger is the left-hand side of equation (33).

For our analysis we draw on the work of Galiotis *et al.*[21], who have investigated the strain dependence of the Raman frequencies of Kelvar 49® fibre, in the range 1100–1700 cm^{-1}, between 0% and 2% axial strain (ε_{33}). From their data, the gradients in frequency appear to be roughly independent of both frequency and strain. The frequencies and peak shifts of six vibrational modes are reproduced in *Table 2*. Hence we assume the simplifications suggested above [(i)–(ii)], i.e. that the second derivatives of frequency with respect to strain are essentially zero, and take an average value for $K_\nu = -3\ cm^{-1}\ \%^{-1}$ (i.e. $-300\ cm^{-1}$). (For this coarse approximation, we do not distinguish between the magnitude of the constant stress derivatives and that of the constant strain derivatives required by equations (31) and (33)). At 298 K, $h\beta = 0.0048$ cm, V_o is 5.26×10^{-22} cm^3 (the unit cell volume), N_o is taken to be the 56 atoms for PPTA (two repeat units or four monomeric units per unit cell) and $(kT/V_oC_{3333}) = 4.66\times10^{-5}$.

Estimation of the Einstein and Debye frequencies of such a material is difficult. Bondi[22] reports Debye temperatures (Θ_D) between 100°C and 400°C for monatomic solids, which corresponds to $\nu_D = k\Theta_D/h$ between 70 cm^{-1} and 280 cm^{-1}. Values for glassy polymers are on the order of 120°C. Unfortunately, there exist no estimates for Debye or Einstein temperatures for polymeric crystals. However, guided by those systems for which data is available, we may presume a conservative value of $\Theta_D = 100$°C and $\Theta_E = 0.75\Theta_D = 75$°C, which corresponds to $\nu_D = 70\ cm^{-1}$ and $\nu_E = 52\ cm^{-1}$. We then obtain:

Einstein approximation:

$$(-3N_o/\beta V_oC_{LMNK})(h\beta K_\nu)^2\{\exp(h\beta\nu_E)/[\exp(h\beta\nu_E)-1]^2\} = -0.259 \quad (34)$$

Debye approximation:

$$-(3N_o/\beta V_oC_{LMNK})(K_\nu^2/h\beta\nu_D^3) \times \int_0^{h\beta\nu_D} x^2\exp(x)/[\exp(x)-1]^2\,dx = -0.143 \quad (35)$$

For both types of approximations, the analysis indicates that the elastic constants are overestimated using potential energy only. The true modulus of PPTA fibres, according to these considerations, is between 74% and 86% of the values computed neglecting thermal motion.

The statistical mechanical considerations presented here, together with the thermodynamic analysis laid out above, leads to the contention that entropic and kinetic energy contributions to the elastic moduli in fibrous polymer crystals are not negligible and may in fact (in aramid fibres) amount to as much as 15–30% of the total response to axial deformation. In the following, we will adhere to calculations of the elastic constants from changes in the potential energy for deformed structures, adjusting these values a posteriori to estimate the 'true' moduli.

METHOD OF CALCULATION

In the case of static crystals fully minimized in potential energy with respect to both intramolecular and intermolecular degrees of freedom, the first order coefficients of equation (5) are all zero (i.e. there is no internal residual stress). To obtain the 21 independent elastic coefficients, C_{LMNK}, 21 deformation 'experiments' need be performed. These were selected as follows: three uniaxial tensions (ε_{LL}); three simple shears (ε_{LM}); three biaxial tensions (ε_{LL}, ε_{MM}); three dual component shears (ε_{LM}, ε_{NK}); and nine combined tension/shear (ε_{LL}, ε_{NK}).

The first two types of deformation require the minimum energy configuration plus two deformed configurations each ($\pm\varepsilon$), from which an estimate of C_{LMNK} may be calculated using a three-point formula for $\partial^2U/\partial\varepsilon_{LM}\,\partial\varepsilon_{NK}$. The other three types each require an additional two deformed configurations (e.g. $+\varepsilon_{LM}$, $+\varepsilon_{NK}$ and $-\varepsilon_{LM}$, $-\varepsilon_{NK}$), which in combination with the previous deformed structures yield estimates of C_{LMNK} through use of a seven-point formula for $\partial^2U/\partial\varepsilon_{LM}\,\partial\varepsilon_{NK}$.

From equations (5) and (8), in the absence of entropic contributions, the elements of the compliance matrix are obtained as

$$C_{LMNK} = (\rho_o/M_{ru})\,\partial^2U/\partial\varepsilon_{LM}\,\partial\varepsilon_{NK} \quad (36)$$

Because of the feature of chain alignment within the model, deformation parallel to the chain propagation direction and lateral to it may not be treated identically. Tensile deformation in the latter case is primarily a function of intermolecular packing parameters and may be imposed by appropriately straining the packing geometry. Tensile deformation along the chain direction is an implicit function of intramolecular parameters and may be imposed by applying a forcing function to cause deformation of the chain axis. On the other hand, simple shear in a plane containing the chain axis may be induced by altering the intermolecular description, while shear in a plane cutting the chain axis is precluded by formulation of the model, which defines the z-axis of the global coordinate system as the alignment direction of the chain axes. In the actual 'experiments' we impose deformation through the application of engineering strain components e_{LM}, which need not compose a symmetric matrix; the resulting rigid body rotations implied by the non-symmetric strain matrices have no bearing on the calculated internal energy of the deformed body. Generalized forms of the engineering strain matrices for one example each of the five imposed deformations are as follows (where the e_{ij} are small values):

Uniaxial tension (x-axis) $\mathbf{e} = \begin{bmatrix} e_{11} & 0 & 0 \\ 0 & 0 & 0 \\ 0 & 0 & 0 \end{bmatrix}$

Simple shear (yz-plane, y-direction) $\mathbf{e} = \begin{bmatrix} 0 & e_{12} & 0 \\ 0 & 0 & 0 \\ 0 & 0 & 0 \end{bmatrix}$

Biaxial tension (*x*-axis, *y*-axis)

$$\mathbf{e}=\begin{bmatrix} e_{11} & 0 & 0 \\ 0 & e_{22} & 0 \\ 0 & 0 & 0 \end{bmatrix}$$

Dual component shear (*yz*-plane, *y*-direction; *yz*-plane, *z*-direction)

$$\mathbf{e}=\begin{bmatrix} 0 & e_{12} & e_{13} \\ 0 & 0 & 0 \\ 0 & 0 & 0 \end{bmatrix}$$

Tension/shear (*x*-axis; *yz*-plane, *y*-direction)

$$\mathbf{e}=\begin{bmatrix} e_{11} & e_{12} & 0 \\ 0 & 0 & 0 \\ 0 & 0 & 0 \end{bmatrix}$$

Equivalent tensorial strain elements may readily be determined (i.e. $\varepsilon_{LL}=e_{LL}$ and $\varepsilon_{LM}=\varepsilon_{ML}=\frac{1}{2}e_{LM}$). By imposing a strain and reminimizing with respect to intramolecular and intermolecular degrees of freedom, we allow the components of the structure to respond in a non-affine manner; this process is conceptually consistent with a realistic interpretation of atomic rearrangement in a system involving bonded and non-bonded atoms.

ELASTICITY OF PPTA

Chain description

The model used for PPTA is a modification of the simple chain description used previously to identify optimal crystal structures[14]. The latter described the single chain using fixed bond lengths, hexagonal planar phenyl rings, and planar sp^2 bond orientations at the amide carbons and nitrogens, requiring only six torsional degrees of freedom and eight valence bond angle degrees of freedom. This chain description is shown in *Figure 1a*. This model contains sufficient 'internal' freedom for the chain to adjust to its preferred packing configuration but is too 'restricted' to respond realistically to strains imposed along the chain axis. In the modified chain description, illustrated in *Figure 1b*, the planarity constraint at the amide nitrogens and carbons is relaxed, resulting in 10 torsional degrees of freedom. The rigid phenylene ring has been replaced by a planar symmetric ring which may be described using only one bond angle and two bond length degrees of freedom. Finally, the bonds in the chain backbone were allowed to respond to deformation, adding six more bond lengths to the degrees of freedom, for a total of 10 bond angle and 10 bond length degrees of freedom for the PPTA repeat unit. Valence force field potentials[11] were introduced to describe the potential energy of these deformations, with the equilibrium positions chosen so as to reproduce the original chain upon energy minimization. *Table 3* shows the correlation between corresponding values for the above-mentioned degrees of freedom at the minimum energy cell configuration for one of the previously calculated PPTA structures (that denoted PPTA structure 3 in ref. 14; this structure is very similar to the PPTA modification I first reported by Northolt[23]) using the two chain descriptions. The intermolecular degrees of freedom remained unchanged (i.e. two periodicity lengths, three periodicity orientation angles, two setting angles and one

Table 3 Comparison of the two chain descriptions used for structure and mechanical property calculations

		For structure calculations	For mechanical property estimation
Number of degrees of freedom		22	38
Bond length[a] (Å)			
$C–C_{ar,1}$	(l_1, l_5)	1.50 (fixed)	1.504, 1.508
$C_{ar,1}–C_{ar,2}$	(l_7, l_9)	1.40 (fixed)	1.404, 1.402
$C_{ar,2}–C_{ar,3}$	(l_8, l_{10})	1.40 (fixed)	1.400, 1.396
C–N	(l_3, l_6)	1.39 (fixed)	1.385, 1.385
$C_{ar,1}$–N	(l_2, l_4)	1.41 (fixed)	1.398, 1.400
Bond angle[a] (degrees)			
$C_{ar,6}–C_{ar,1}–C_{ar,2}$	(θ_9, θ_{10})	120 (fixed)	119.4, 120.3
$C_{ar,1}$–C=O	(θ_2)	118.9	118.9
N–C=O	(θ_8)	119.2	119.3
$C_{ar,1}$–C–N	(θ_1, θ_7)	122.0, 121.9	121.8, 122.0
C–N–H	(θ_4)	123.1	119.0
$C_{ar,1}$–N–H	(θ_6)	118.4	118.1
$C_{ar,1}$–N–C	(θ_3, θ_5)	123.1, 122.7	122.9, 122.6
Bond torsion (degrees)			
$C_{ar,2}–C_{ar,1}–C–N$	(ϕ_1, ϕ_3)	−26.0, −153.7	−25.7, −159.0
$C_{ar,2}–C_{ar,1}–C=O$	(ϕ_2)	$(\phi_3+180°)$	19.0
$C_{ar,1}–N–C=O$	(ϕ_9)	$(\phi_{10}+180°)$	172.0
$C_{ar,1}–C–N–C_{ar,1'}$	(ϕ_5, ϕ_{10})	5.6, −6.6	5.8, −6.9
$C_{ar,2}–C_{ar,1}–N–C$	(ϕ_6, ϕ_8)	−137.3, −43.1	−134.6, −44.4
$C_{ar,2}–C_{ar,1}–N–H$	(ϕ_7)	$(\phi_8+180°)$	137.8
$C_{ar,1}–C–N–H$	(ϕ_4)	$(\phi_5+180°)$	−167.8
Intermolecular[b]			
A (Å)		4.78	4.78
B (Å)		4.90	4.93
α (degrees)		90.3	89.7
β (degrees)		89.9	89.5
γ (degrees)		62.1	61.5
ω_1 (degrees)		101.4	99.5
ω_2 (degrees)		−79.5	−81.4
f_2		0.45	0.45
Density (g cm^{-3})		1.46	1.46
Cohesive energy (kcal mol^{-1})		38.3	37.8

[a] Refer to *Figure 1* for explanation of symbols

[b] The precise meanings of these intermolecular parameters have been previously explained in detail in reference 14

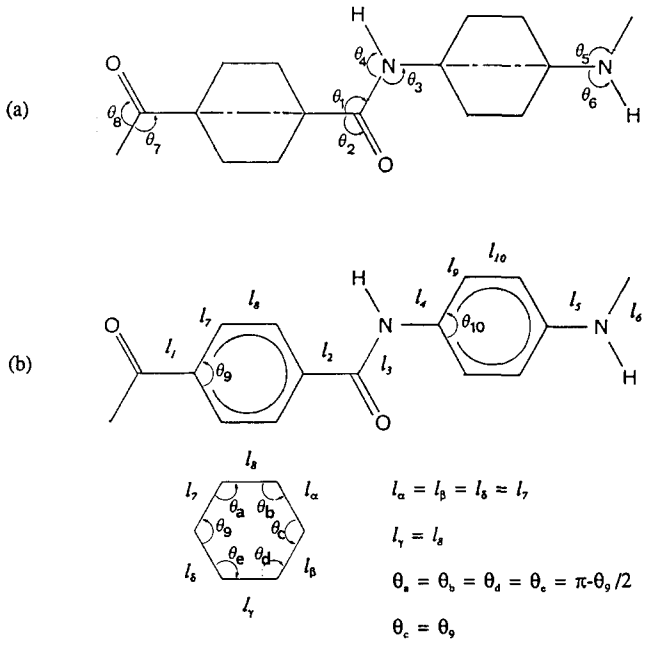

Figure 1 Segment of PPTA with all torsion angles in their zero positions. (a) Type I chain description for determination of multichain packing behaviour. (b) Type II chain description for determination of mechanical properties

translational displacement). The cohesive energy of this structure calculated using the second chain description is within 2.1 kJ mol^{-1} of that obtained using the simpler description; this lends further confidence to the accuracy and adequacy of the simpler version for structure and cohesive energy calculations.

It remains to define the coordinate axes of mechanical deformation: the x_3-axis of deformation corresponds to the c-axis of the pseudocrystal, along which the chain axes are aligned; the x_1–x_3 plane contains the ac-facet of the pseudocrystal wherein lie the hydrogen-bonded sheets; the x_2-axis and the bc-facet are defined by orthogonality and crystal periodicity relationships, respectively.

Determination of crystallite compliance and stiffness matrices

The first structure considered is that denoted[14] PPTA structure 3. Initially, the multichain structure was subjected to $\pm 0.4\%$ tensile strains along the crystallographic c-axis (the chain axis), with all other internal and external degrees of freedom allowed to adjust (i.e. a 'constant pressure' deformation). The resulting E_{33} modulus is 303 GPa; the resulting densities of the strained structures deviated from the strain free value by $\pm 0.16\%$, indicative of a slight dilation (compression) of the lattice upon extension (compression).

In a second set of experiments, the full complement of 21 deformations was performed, allowing only degrees of freedom internal to the unit cell to relax (i.e. the optionally strained lattice dimensions a, b, c and interaxial angles α, β and γ were fixed). The complete stiffness matrix is presented below (eqn. (41)) in the 6×6 Voigt format. In this convention, only one subscript is required to identify the appropriate element of stress or strain, and two for the corresponding stiffness and compliance matrices (e.g. $\varepsilon_L = \varepsilon_{LL}$ for $L = 1, 2, 3$; and $\varepsilon_4 = 2\varepsilon_{23}$, $\varepsilon_5 = 2\varepsilon_{13}$, $\varepsilon_6 = 2\varepsilon_{12}$). The magnitudes of imposed strains were selected to be large enough to give numerically significant differences in potential energy (i.e. $e_L = 0.4\%$ for $L = 3$ and 0.8% for $L = 1, 2$; $e_L = 1.6\%$ for $L = 4, 5, 6$); larger imposed deformations tax the validity of the assumption of material elasticity and the utility of the simple three- and seven-point approximation formulae. Deformations imposed by e_{33} and e_{23}, representing roughly the extremes of the range of elastic response, were checked for various strain levels; the calculated stiffness elements remained consistent up to 3.2% strain or higher. Up to 1.6% deformation, removal of the imposed deformation and reminimization of potential energy with respect to the internal coordinate degrees of freedom gives back the original undeformed configuration, ensuring that the strain levels employed are within the domain of elastic response. The resulting precision in the reported values are on the order of $\pm 5\%$, or ± 1–5 GPa.

The compliance matrix is calculated by inversion of the stiffness matrix:

$$\mathbf{S} = \mathbf{C}^{-1} \tag{37}$$

From the compliance matrix are calculated the Young's moduli E_i, the shear moduli G_i, and the first six Poisson's ratios ν_{ij}:

$$E_i = 1/S_{ii}; \qquad i = 1, 2, 3 \tag{38}$$

$$G_j = 1/S_{ii}; \qquad i = 4, 5, 6 \text{ and } j = i - 3 \tag{39}$$

$$\nu_{ij} = -S_{ij}/S_{jj}; \qquad i, j = 1, 2, 3 \tag{40}$$

The full stiffness and compliance matrices and the derived moduli are found to be:

$$\mathbf{C} = \begin{bmatrix} 40 & 23 & 13 & 0.1 & 1.2 & 2.4 \\ & 31 & 41 & 1.5 & 3.2 & 1.9 \\ & & 360 & 0.3 & 5.0 & 11 \\ & & & 5.5 & 3.7 & 2.7 \\ & & & & 22 & 3.2 \\ & & & & & 7.5 \end{bmatrix} \text{GPa} \tag{41}$$

$$\mathbf{S} = \begin{bmatrix} 4.8 & -4.2 & 0.35 & 1.8 & 0.21 & -1.8 \\ & 7.5 & -0.74 & -2.5 & -0.52 & 1.7 \\ & & 0.37 & 0.50 & 0.02 & -0.66 \\ & & & 25 & -2.8 & -8.5 \\ & & & & 5.3 & -1.2 \\ & & & & & 18 \end{bmatrix} \times 10^{-2}\ \text{GPa}^{-1} \tag{42}$$

$$\begin{array}{lll} E_1 = 21 \text{ GPa} & E_2 = 13 \text{ GPa} & E_3 = 270 \text{ GPa} \\ G_1 = 4.0 \text{ GPa} & G_2 = 19 \text{ GPa} & G_3 = 5.6 \text{ GPa} \\ \nu_{12} = 0.55 & \nu_{21} = 0.86 & \nu_{13} = -0.94 \\ \nu_{31} = -0.07 & \nu_{23} = 2.01 & \nu_{32} = 0.10 \end{array} \tag{43}$$

The obvious trends to be noted here are that the transverse moduli E_1 and E_2 are roughly 5–8% of the axial modulus E_3. As was suggested previously from a detailed consideration of structural energetics[14], the two transverse moduli are of comparable magnitude; E_1 is slightly larger than E_2 due to the stretching of hydrogen bonding interactions in the former. The value calculated for G_2 is comparable to that of E_1 and is indicative of the expected resistance to shear deformation of the hydrogen-bonded sheet structure. The shear moduli G_1 and G_3, corresponding to motions of the hydrogen-bonded sheets of chains parallel and perpendicular, respectively, to the chain axes, are roughly 1–2% of the axial modulus. The complete stiffness and compliance matrices are positive definite and satisfy the requirement for positive strain energy[24] (i.e. $\Psi = \boldsymbol{\varepsilon}^T \boldsymbol{C} \boldsymbol{\varepsilon} = \boldsymbol{\sigma}^T \boldsymbol{S} \boldsymbol{\sigma} > 0$) for an arbitrary small deformation imposed by ε or σ.

Estimations for alternative allomorphs

At least one other crystal allomorph has been isolated by precipitation from acid solution into water under controlled conditions of polymer concentration and post-precipitation heat treatment[25]. Other energetically stable packing geometries may also exist to lesser extents in the actual polymer fibre. In consideration of these possibilities, we repeated the above procedure for two additional structures suggested by the model analysis. Structure 4 of reference 14 closely resembles structure 3 in its unit cell geometry, with the distinction that amide dipoles in register in neighbouring sheets of hydrogen-bonded chains are alternating in direction. Structure 5 of reference 13 represents that calculated geometry which most closely approximates the second crystal polymorph reported in the literature. (However, it should be noted that none of the model structures derived by minimization of total potential energy replicate

this reported structure to the extent that structure 3 resembles modification I.) Shown below is a summary of the stiffness and compliance matrices for these two PPTA structures; in each case, these matrices satisfy the requirement of positive strain energy of deformation:

PPTA structure 4:

$$\mathbf{C}=\begin{bmatrix} 55 & 30 & 0.5 & 1.4 & 7.2 & 0.4 \\ & 33 & 26 & -7.7 & -6.4 & 4.0 \\ & & 390 & -9.6 & -10 & 3.1 \\ & & & 19 & -5.2 & 2.4 \\ & & & & 22 & -3.0 \\ & & & & & 19 \end{bmatrix} \text{GPa} \quad (44)$$

$$\mathbf{S}=\begin{bmatrix} 12 & -16 & 0.5 & -10 & -10 & 2.6 \\ & 24 & -0.8 & 15 & 15 & -4.2 \\ & & 0.3 & -0.3 & -0.3 & 0.1 \\ & & & 15 & 11 & -3.1 \\ & & & & 15 & -1.9 \\ & & & & & 6.1 \end{bmatrix} \times 10^{-2}\ \text{GPa}^{-1} \quad (45)$$

$$\begin{aligned} &E_1=8.5\ \text{GPa} && E_2=4.1\ \text{GPa} && E_3=350\ \text{GPa} \\ &G_1=6.9\ \text{GPa} && G_2=6.9\ \text{GPa} && G_3=16\ \text{GPa} \\ &\nu_{12}=0.6 && \nu_{21}=1.3 && \nu_{13}=2.7 \\ &\nu_{31}=-0.04 && \nu_{23}=0.03 && \nu_{32}=0.03 \end{aligned} \quad (46)$$

PPTA structure 5:

$$\mathbf{C}=\begin{bmatrix} 55 & 18 & 0.6 & 18 & 9.1 & -4.9 \\ & 60 & 12 & 2.0 & 1.9 & -2.9 \\ & & 290 & 9.0 & 36 & 30 \\ & & & 9.4 & 1.5 & 2.6 \\ & & & & 20 & -2.4 \\ & & & & & 20 \end{bmatrix} \text{GPa} \quad (47)$$

$$\mathbf{S}=\begin{bmatrix} 8.7 & -2.0 & -0.8 & -17 & -3.6 & 2.4 \\ & 2.2 & -0.3 & 3.5 & 1.0 & 0.0 \\ & & 0.7 & -1.6 & -1.5 & -0.8 \\ & & & 44 & 6.1 & -6.1 \\ & & & & 9.0 & 1.8 \\ & & & & & 7.7 \end{bmatrix} \times 10^{-2}\ \text{GPa}^{-1} \quad (48)$$

$$\begin{aligned} &E_1=12\ \text{GPa} && E_2=45\ \text{GPa} && E_3=150\ \text{GPa} \\ &G_1=2.3\ \text{GPa} && G_2=11\ \text{GPa} && G_3=13\ \text{GPa} \\ &\nu_{12}=0.9 && \nu_{21}=0.2 && \nu_{13}=-1.2 \\ &\nu_{31}=-0.1 && \nu_{23}=0.5 && \nu_{32}=0.1 \end{aligned} \quad (43)$$

Significant differences between the elastic properties of these different crystalline microstructures is suggestive of the considerable variation in observable behaviour for PPTA where different or mixed forms are present. The variation in tensile modulus, for example, would be contingent upon the details of chain conformation, which in turn depends upon the intermolecular forces impinging upon the chain from neighbouring units.

Isolated chain compliance and comparison to crystallite compliance

For comparison to calculations in the literature, the isolated chain was also subjected to fixed axial strains of $\pm 0.4\%$, which yielded a chain modulus of 195 GPa. By comparison, Tashiro *et al.*[11] calculated a value of 182 GPa for the isolated chain modulus (referred to there as the crystallite modulus). Fielding-Russell[26] obtained a value of 200 GPa for the all-*trans* planar conformation. The observed tensile modulus falls in the range 120–200 GPa[11,27–29]. It is significant that whereas the tensile stiffness C_{3333} calculated for the single chain is in good agreement with previous estimates, that estimated for the packed structure is considerably higher, in both variable and constant strain simulations (i.e. 303 and 360 GPa, respectively). This is especially puzzling in light of the widespread notion that chain packing should have no significant effect on C_{3333}, since the interactions contributed by the lattice act essentially perpendicular to the chain axis[12,30]. In order to determine the source of this difference, the component breakdowns of energy contributions in both the single chain and packed chain estimations were computed. For this purpose, the intramolecular contribution was defined as that change in energy attributable to changes in intramolecular variables upon deformation, which includes bond stretching, bond angle bending, torsion angle rotation, intramolecular van der Waals interactions and intramolecular Coulombic interactions. For the packed structure, intermolecular interaction contributions were defined as changes upon deformation attributable to intermolecular van der Waals and Coulombic interactions. The contributions to changes in energy upon $\pm 0.4\%$ strain along the *c*-axis (the chain axis) are shown in *Table 4*.

Study of these values in the case of the isolated chain indicates that the minimum energy conformation is the result of a balance between interactions tending to promote chain contraction (i.e. bonds and valence angles) and others promoting chain elongation (i.e. torsions and non-bonded interactions); thus small deformations are accompanied by trade-offs in these interactions. In the packed chain structure, however, the presence of intermolecular interactions greatly alters the balance. Due to impinging intermolecular interactions, the chain conformation is no longer the minimum energy conformation represented by the isolated chain, and as a result the trade-off between intramolecular contributions concurrent with axial strain are no longer balanced, but tend to pay a higher penalty for extension than witnessed previously. On the other hand, intermolecular interactions, primarily the Coulombic interactions, actually favour extension, thus offsetting the higher penalty for conformational extension. This trend may be understood as follows: extension leads to a net separation of atom centres, which decreases the cohesive energy contributions due to van der Waals interactions. However, charge interactions in the packed structure are not randomly oriented, but are so arranged such that attractive interactions predominate. In particular, species of opposite charge are preferentially located closer

Table 4 Partitioning of strain energy (kcal mol^{-1}) among the degrees of freedom of the structure for isolated chain and packed chain simulations

Tensile strain (%)	ΔE_{bond}	ΔE_{angl}	ΔE_{tors}	ΔE_{vdW}	ΔE_{Coul}		
Isolated chain							
Intramolecular							
						ΔE_{intra}	
+0.4	0.43	0.46	−0.21	−0.60	−0.007	0.078	
−0.4	−0.24	−0.34	0.58	0.002	0.037	0.042	
Packed chains							
Intramolecular							
						ΔE_{intra}	
+0.4	0.42	0.49	−0.007	−0.69	−0.022	0.19	
−0.4	−0.33	−0.39	0.093	0.65	0.040	0.061	
Intermolecular							
						ΔE_{inter}	ΔE_{total}
+0.4	–	–	–	0.030	−0.10	−0.074	0.12
−0.4	–	–	–	−0.032	0.075	0.042	0.10

together. Even an affine extension imposes larger absolute changes in charge separation for those species which are farther apart, i.e. species of like charge, resulting in a net improvement of the total Coulombic interaction. Non-affine deformations such as performed here will probably be even more preferential in distributing charge separation. In the sum, both intra- and intermolecular interactions contribute to resist compression, while the advantages gained in intermolecular interaction only partially offset the resistance of chain conformation to extension. The net result is the increase in the stiffness constant C_{3333}. This illustrates not only the importance of intermolecular contributions to resistance to deformation, but the complexity of changes in intramolecular response which accompany the changes in conformation that result from interactions with neighbouring chains. The computed variation of E_3 with crystal structure witnessed above (the values span a factor of 2.2) is clear indication of the importance of packing even on C_{3333}.

FIBRE MODULI

Derivation of fibre symmetry relations

One may derive estimates for the moduli of the polycrystal mosaic present in the fibre from the complete elastic constant matrices by applying assumptions concerning the crystal packing morphology and the distribution of stress and strain over the packed crystals. For this purpose, we treat the fibre as a polycrystalline structure possessing perfect alignment of the molecular axes along the fibre axis, but random orientation of the crystals in the planes lateral to the fibre axis. We also ignore the effects of any inter-crystalline matrix material. Assuming that an imposed strain is uniform for all elements of the polycrystalline fibre, one may calculate the fibre stiffness matrix as the cylindrical average of the crystalline stiffness matrix. This matrix is inverted to obtain the fibre compliance matrix and the elastic moduli as previously described; this procedure yields the volume average of stiffnesses, or Voigt limit, which provides an upper bound to the estimation of elastic constants. Alternatively, one may assume that stress, rather than strain, is uniform, resulting in the analogous volume average of compliances, or Reuss limit. These two assumptions, while neither being exactly correct, provide the upper and lower limits to the elastic constants for the cylindrically symmetric polycrystal 'composite', within which the true elastic constants must lie[31].

For the case of fibre symmetry the contribution to compliance from an individual crystal is expressed as a function of crystal orientation (Ω denotes the angular position of the crystal) in tensorial form as:

$$\mathbf{C}_\Omega = \mathbf{T}_\Omega \mathbf{T}_\Omega \mathbf{C} \mathbf{T}_\Omega^T \mathbf{T}_\Omega^T \tag{50}$$

where $\mathbf{T}_\Omega$ is the rotation matrix (for the fibre axis parallel to the z direction):

$$\mathbf{T}_\Omega = \begin{bmatrix} \cos\Omega & \sin\Omega & 0 \\ -\sin\Omega & \cos\Omega & 0 \\ 0 & 0 & 1 \end{bmatrix} \tag{51}$$

Denoting the column array of the elements of a matrix as $\{\ \}_{col}$, the elements being arranged in 'reading' order, i.e. by rows, and using $\otimes$ to signify the direct matrix product, one may rewrite equation (50) for $\mathbf{C}_\Omega$ as:

$$\{\mathbf{C}_\Omega\}_{col} = (\mathbf{T}_\Omega \otimes \mathbf{T}_\Omega \otimes \mathbf{T}_\Omega \otimes \mathbf{T}_\Omega)\{\mathbf{C}\}_{col} \tag{52}$$

or, using the reduced notation[32] where $\mathbf{T}^{xp}$ indicates the self-direct product of degree p of the matrix $\mathbf{T}$

$$\{\mathbf{C}_\Omega\} = \mathbf{T}_\Omega^{x4}\{\mathbf{C}\} \tag{53}$$

Then the cylindrical average over Ω becomes:

$$\langle\{\mathbf{C}_\Omega\}\rangle = (1/2\pi)\int_0^{2\pi} \mathbf{T}_\Omega^{x4}\{\mathbf{C}\}\,d\Omega = \langle\mathbf{T}_\Omega^{x4}\rangle\{\mathbf{C}\} \tag{54}$$

Upon integration, one obtains 41 non-zero terms in $\langle\mathbf{T}_\Omega^{x4}\rangle$, of which 21 are independent. Taking advantage of the symmetries in $\mathbf{C}$, one can derive simple equations for the six independent terms of the cylindrically averaged stiffness matrix $\langle\mathbf{C}_\Omega\rangle$, which may be collected into Voigt form as shown below:

$$\langle\mathbf{C}_\Omega\rangle = \begin{bmatrix} A & B & C & & & \\ B & A & C & & 0 & \\ C & C & F & & & \\ & & & E & & \\ & 0 & & & E & \\ & & & & & D \end{bmatrix} \quad \text{Voigt average} \tag{55}$$

where

$$A = (1/8)(3C_{11} + 3C_{22} + 2C_{12} + 4C_{66})$$

$$B=(1/8)(C_{11}+C_{22}+6C_{12}-4C_{66})$$
$$C=(1/2)(C_{13}+C_{23})$$
$$D=(1/8)(C_{11}+C_{22}-2C_{12}+4C_{66})$$
$$E=(1/2)(C_{44}+C_{55})$$
$$F=C_{33}$$

Similarly, the cylindrically averaged compliance matrix may be expressed as:

$$\langle S_\Omega \rangle = \begin{bmatrix} A & B & C & & & \\ B & A & C & & 0 & \\ C & C & F & & & \\ & & & E & & \\ & 0 & & & E & \\ & & & & & D \end{bmatrix} \quad \text{Reuss average} \qquad (56)$$

where

$$A=(1/8)(3S_{11}+3S_{22}+2S_{12}+S_{66})$$
$$B=(1/8)(S_{11}+S_{22}+6S_{12}-S_{66})$$
$$C=(1/2)(S_{13}+S_{23})$$
$$D=(1/2)(S_{11}+S_{22}-2S_{12}+S_{66})$$
$$E=(1/2)(S_{44}+S_{55})$$
$$F=S_{33}$$

Voigt and Reuss limits for PPTA

Applying this approach to the crystallographic stiffness and compliance matrices given previously, one obtains the upper (Voigt) and lower (Reuss) limits for the fibre elastic constants. In *Table 5*, these constants are listed for PPTA structure 3. Also shown are the available experimentally determined moduli for PPTA (Kevlar) fibres, as well as the results of calculations reported by Northolt and van Aartsen using bond deformation models[12]. Values for G_3 and ν_{31} are not independent, but may be determined easily by the relations:

$$G_3=\tfrac{1}{2}E_1/(1+\nu_{12}) \qquad (57)$$
$$\nu_{31}=\nu_{13}E_1/E_3 \qquad (58)$$

The values calculated for the PPTA structure 3 exhibit considerable spread between the upper (Voigt) and lower (Reuss) bounds. The values for all moduli tend to be somewhat higher than the experimentally measured values. This may be expected due to the idealization of orientation and crystallite packing in the calculated estimates, as well as likely defects and structural imperfection which would lower the experimentally determined values from their theoretical maxima. After taking into consideration entropic corrections, the calculated lower bounds for E_3 and G_1 may be as low as 220 and 4.1 GPa, respectively, in excellent agreement with experimental values.

Table 6 lists the fibre moduli calculated for two additional predicted structures of PPTA (structures 4 and 5). One observes the consistent trend in moduli: $E_3>E_1>G_1$. The differences in the values for the predicted moduli of each structure again suggest the potential for considerable variation in bulk properties, contingent upon the polymorphic composition of each sample.

Table 5 PPTA fibre elastic constants (GPa): theoretical (structure 3) and experimental

	Voigt	Reuss	Predicted range[a]	Experiment	Northolt[b]
Extensional modulus (E_3)	330	270	220–290	120–200[c–f]	220
Transverse modulus (E_1, E_2)	22	6.6	5.2–19	–	16–29[g]
Torsional modulus (G_1, G_2)	14	5.2	4.1–12	2[c], 0.95–2.2[h]	2.5–5.7[g]
Extensional Poisson's ratio (ν_{13}, ν_{23})	0.46	0.54	–	–	–
Transverse Poisson's ratio (ν_{12}, ν_{21})	0.60	0.66	–	–	–

[a] After correction for entropy contributions, upper bound is 87% of the Voigt limit and lower bound is 79% of the Reuss limit
[b] From Northolt and van Aartsen[12]
[c] From Allen[29]
[d] From Tashiro *et al.*[11]
[e] From Gaymans *et al.*[27]
[f] From Kwolek *et al.*[28]
[g] Based on the assumption that linear hydrogen bonds are the dominant interactions between chains
[h] From Knoff[33]

Table 6 PPTA fibre theoretical elastic constants (GPa): structures 4 and 5

	Structure 4			Structure 5		
	Voigt	Reuss	Predicted range[a]	Voigt	Reuss	Predicted range[a]
Extensional modulus (E_3)	390	350	270–340	290	150	120–250
Transverse modulus (E_1, E_2)	39	7.9	6.2–34	52	22	17–45
Torsional modulus (G_1, G_2)	20	6.7	5.3–18	15	3.8	3.0–13
Extensional Poisson's ratio (ν_{13}, ν_{23})	0.2	2.1	–	0.1	−0.3	–
Transverse Poisson's ratio (ν_{12}, ν_{21})	0.5	0.8	–	0.3	0.2	–

[a] After correction for entropy contributions, upper bound is 87% of the Voigt limit and lower bound is 79% of the Reuss limit

CONCLUSIONS

In a previous paper, we have employed the methods of molecular mechanics for a detailed study of the solid state structure of PPTA, a stiff chain polymer. From these results, we have now performed deformation 'experiments' of the minimum potential energy structures in order to simulate the elastic response of the polymer pseudocrystal. These calculations provide the necessary information to estimate the elastic moduli of both the single crystal and the oriented fibre in the limits of uniform stress and uniform strain throughout the fibre. Calculations for several polymorphs of PPTA suggest that elastic behaviour depends strongly upon the details of the crystal structure. Our computations suggest that the large intermolecular interactions present in the PPTA system can have a significant effect on the longitudinal as well as the transverse moduli, resulting in considerable discrepancy between the results of single chain and packed chain estimation procedures. It also appears, based on simple estimation procedures using the limited available experimental data, that entropic contributions to the elastic moduli at room temperature are significant and contribute to a downward adjustment of the theoretical elastic constants; for the tensile modulus of the fibre they are $\sim$15–30% of the total value. The apparent success of single chain calculations to estimate the fibre modulus are, in our judgement, the result of compensation of the considerable effects of two simplifications: the neglect of packing interactions, which leads to underestimation of the modulus, and neglect of the contributions of entropy, or thermal motion, which leads to overestimation.

ACKNOWLEDGEMENTS

The authors gratefully acknowledge the support of a Graduate Fellowship to G.C.R. from the National Science Foundation and financial assistance from the Schweizerische Nationalfonds zur Föderung der Wissenschaftlichen Forschung (NF Sektion II).

REFERENCES

1 Anand, J. N. *J. Macromol. Sci. Phys.* 1967, **B1**, 445
2 McCullough, R. L. *J. Macromol. Sci. Phys.* 1974, **B9**, 97
3 Tashiro, K., Kobayashi, M. and Tadokoro, H. *Macromolecules* 1978, **11**, 908
4 Tashiro, K., Kobayashi, M. and Tadokoro, H. *Macromolecules* 1978, **11**, 914
5 Tashiro, K. and Tadokoro, H. *Macromolecules* 1981, **14**, 781
6 Tripathy, S. K., Hopfinger, A. J. and Taylor, P. L. *J. Phys. Chem.* 1981, **85**, 1371
7 Sorensen, R. A., Liau, W. B. and Boyd, R. H. *Macromolecules* 1988, **21**, 194
8 Sorensen, R. A., Liau, W. B., Kesner, L. and Boyd, R. H. *Macromolecules* 1988, **21**, 200
9 Hummel, J. P. and Flory, J. P. *Macromolecules* 1980, **13**, 479
10 Erman, B., Flory, J. P. and Hummel, J. P. *Macromolecules* 1980, **13**, 484
11 Tashiro, K., Kobayashi, M. and Tadokoro, H. *Macromolecules* 1977, **10**, 413
12 Northolt, M. G. and Van Aartsen, J. J. *J. Polym. Sci., Polym. Symp. Edn.* 1977, **58**, 283
13 Saruyama, Y. and Miyaji, H. *J. Polym. Sci., Polym. Phys. Edn.* 1985, **23**, 1637
14 Rutledge, G. C. and Suter, U. W. *Macromolecules* 1991, **24**, 1921
15 Weiner, J. H. 'Statistical Mechanics of Elasticity', Wiley-Interscience, New York, 1983
16 Theodorou, D. N. and Suter, U. W. *Macromolecules* 1986, **19**, 139
17 Ii, T., Tashiro, K., Kobayashi, M. and Tadokoro, H. *Macromolecules* 1986, **19**, 1772
18 Ii, T., Tashiro, K., Kobayashi, M. and Tadokoro, H. *Macromolecules* 1986, **19**, 1809
19 Ii, T., Tashiro, K., Kobayashi, M. and Tadokoro, H. *Macromolecules* 1987, **20**, 347
20 McQuarrie, D. A. 'Statistical Mechanics', Harper and Row, New York, 1976
21 Galiotis, C., Robinson, I. M., Young, R. J., Smith, B. J. E. and Batchelder, D. N. *Polym. Commun.* 1985, **26**, 354
22 Bondi, A. 'Physical Properties of Molecular Crystals, Liquids, and Glasses', John Wiley and Sons, New York, 1968
23 Northolt, M. G. *Eur. Polym. J.* 1974, **10**, 799
24 Nye, J. F. 'Physical Properties of Crystals', Clarendon Press, Oxford, 1985
25 Haraguchi, K., Kajiyama, T. and Takayanagi, M. *J. Appl. Polym. Sci.* 1979, **23**, 915
26 Fielding-Russell, G. S. *Text. Res. J.* 1971, **41**, 861
27 Gaymans, R. J., Tijssen, J., Harkema, S. and Bantjes, A. *Polymer* 1976, **17**, 517
28 Kwolek, S., Memeger, W. and Van Trump, J. E. 'International Symposium on Polymers for Advanced Technology' (Ed. M. Lewin), IUPAC, VCH Publishers, Weinheim, 1987, p. 421
29 Allen, S. R. *Polymer* 1988, **29**, 1091
30 Holliday, L. and White, J. W. *Pure Appl. Chem.* 1971, **26**, 545
31 Arridge, R. G. C. 'An Introduction to Polymer Mechanics', Taylor and Francis, London, 1985
32 Flory, P. J. *Macromolecules* 1974, **7**, 381
33 Knoff, W. E. *J. Mater. Sci. Lett.* 1987, **6**, 1392